Journal of Molecular Liquids 306 (2020) 112804

Contents lists available at ScienceDirect

Journal of Molecular Liquids

journal homepage: www.elsevier.com/locate/molliq

Density, viscosity, surface tension and intermolecular interaction of triethylene glycol and 1,2-diaminopropane binary solution & its potential downstream usage for bioplastic production

Xiaoqian Jia, Shuai Zhang, Bin Li, Jinrong Yang, Jianbin Zhang *, Jilagamazhi Fu *

College of Chemical Engineering, Inner Mongolia University of Technology, Hohhot 010051, China
Inner Mongolia Engineering Research Center for CO_2 Capture and Utilization, Hohhot 010051, China

ARTICLE INFO

Article history:
Received 13 January 2020
Received in revised form 26 February 2020
Accepted 28 February 2020
Available online 05 March 2020

Keywords:
Density
Viscosity
Triethylene glycol
1,2-Diaminopropane
CO_2-storage-material
Poly-β-hydroxybutyrate

ABSTRACT

In this work, triethylene glycol (TEG) and 1,2-diaminopropane (DAP) binary mixture was proposed as a novel CO_2 capturing solution. In order to understand the binary system better, the key physical and chemical properties of TEG and DAP binary solution including the density, viscosity and surface tension were determined and analyzed. The excess molar volume (V_m^E), viscosity deviation ($\Delta\eta$) and surface tension deviation ($\Delta\gamma$) of the solution were calculated and fitted by Redlich-Kister (R-K) equation to evaluate the factor and standard deviations between the experimental and calculated quantities. Meanwhile, the as-determined UV–Vis, FTIR, and Fluorescence spectra suggested that intermolecular hydrogen bonds were formed within the binary solution. In term of the excess molar volume, the intermolecular bonds were closely formed when the molar ratio of TEG to DAP was at 1: 1. This system showed strong CO_2 capture capability, in which about 0.34 g CO_2 was absorbed by per gram of DAP and TEG system. The resulting CO_2-Storage Material (CO_2SM) was further applied as potential carbon source for Poly-β-hydroxybutyrate (PHB, bioplastic) production by a photoautotrophic-cyanobacterium, and intracellular content of 12.92 wt% was achieved. This work used new biological methods to convert CO_2, the fundamental, physical and chemical properties of the alcohol-amine system were studied, further, the basic data as the reference were provided for PHB downstream synthesis optimization.

1. Introduction

Since middle of the 20th century, CO_2 was considered as major greenhouse gas that causes global warming [1]. After that, CO_2 capture was one of the central strategies to reduce greenhouse gas emissions [2,3]. Because of the low partial pressure of CO_2 after combustion, physical solvent and membrane capture have their innate limitations for large scale application. In comparison, chemical solution possesses higher CO_2 absorption capacity [4].

At present, the most commonly used chemical absorbents were amines which have high efficiency to remove acidic gases from the atmosphere [5]. However, amines are volatile, toxic and costly to produce, which limit its utilization [6]. Therefore, finding ideal solvents with well thermal stability, better CO_2 absorption performance, and less environmental pollution are focused [7,8]. Previous works showed that through adding certain organic solvent, such as ethylene glycol (EG) and diethylene glycol (DEG), the volatility of the amine has dramatically reduced, and the resulting amine-alcohol binary systems showed superior CO_2 absorption capacity [9,10]. Comparing to EG and DEG, triethylene glycol (TEG) absorbs more acidic gases and easy to regenerate [11]. Moreover, the boiling point of TEG was higher than EG and DEG [12]. Thus, TEG could be used as an alternative to previous organic solvents used in binary solution for CO_2 capture. Another issue related to chemical absorbents was that the CO_2 absorbing process was often highly energy-consuming, thus recycling and reutilization of the absorption material became the mainly research topic for sustainable development [13].

PHB was a bioplastic that widely considered as an alternative to conventional plastic such as polyethylene due to its biodegradability [14]. Valorization of industrial fuel gas into value-added product, such as PHB, had great potential of reducing the high production cost of the bioplastic. In addition, high CO_2 capturing and storing potential of amine-alcohol binary system may increase the mass transfer of CO_2 to photoautotroph in alkalinous medium [15], which was usually a limiting factor for PHB biosynthesis under photoautotrophic condition.

In this work, we have tested the CO_2 capturing capacity of a novel amine-alcohol binary solution, namely DAP-TEG, and the system was further applied for PHB production after CO_2 absorption. To our best knowledge, this was the first time that amine-alcohol binary derived system was reported for bioplastic production. Furthermore, in order

* Corresponding authors at: College of Chemical Engineering, Inner Mongolia University of Technology, Hohhot 010051, China.
E-mail addresses: tadzhang@pku.edu.cn (J. Zhang), umfu23@myumanitoba.ca (J. Fu).

https://doi.org/10.1016/j.molliq.2020.112804
0167-7322/

to de-fold the key property of the binary system and possible intermolecular interaction of the components, the parameters of the TEG + DAP binary system including density, dynamic viscosity and surface tension were measured between 293.15 K–318.15 K. The formation of intermolecular bonds was evaluated using UV–Vis, FTIR, and fluorescence spectral technologies. These base data could lay a solid foundation for further understanding and optimization of CO_2 absorption capacity, and therefore PHB production in the downstream. About 0.34 g CO_2 was absorbed by per gram of TEG + DAP system, the resulting CO_2SM was further applied as potential carbon source for PHB (bioplastic) production by a photoautotrophic-cyanobacterium, and intracellular content of 12.92 wt% was achieved.

2. Materials and methods

2.1. Materials

DAP (CAS No.78–90-0, 99% purity) and TEG (CAS No.112–27-6, 99.5% purity) were purchased from Shanghai Macklin Biochemical Co, Ltd. The DAP was further purified through 0.4 Å molecular sieves. The ethanol solution was purchased from the Tianjin Reagent Company. Redistilled water of 0.1 mS cm^{-1} was used to correct gravity bottle and viscometer. All materials used in this research were displayed in Table 1.

2.2. Methods

2.2.1. Preparation of the alcohol-amine binary solution

The binary solution of DAP and TEG were prepared by directly mixing two chemicals, and the weight of two chemicals was measured by analytical balance with accuracy of ±0.1 mg (Sartorius BS224S). Twenty-one groups of mixed alcohol-amine solutions with different mole fractions of two chemicals were prepared. The variations in total weight of the different binary solutions were limited to ±0.3 mg.

2.2.2. Density of the alcohol-amine binary solution

The density of the binary system was measured by a 25 cm^3 gravity bottle. The gravity bottle filled with the binary solvent solution was placed in a water bath kept at six different temperature (precision: ± 0.01 K) for at least 20 min prior to measure the density of the binary solution. Gravity bottle was validated using double-distilled water. The density of each binary mixed solution was measured at least three times, then the closet three values with variation with ±0.0003 g were used to calculate the average density for each binary mixed solution. The equation for calculation the density (ρ) of binary solution as Eq. [1]:

$$\rho = m/V \tag{1}$$

where m is the weight of the binary solution, and V is a fixed value of 25 cm^3.

2.2.3. Viscosity of the alcohol-amine binary solutions

The viscosity of the binary solutions was measured by an Ubbelohde capillary viscometer which was corrected by double-distilled water and ethanol (HPLC grade) prior to measurement. The viscometer filled with the binary solution was placed in a water bath at six different temperature (precision: ± 0.01 K) for 20 min prior to the measurement. The flow time of the binary solutions was were measured at least thirteen times, and thirteen approximate values which deviation was ±0.03 s. The following equation was used to calculate kinematic viscosity [2]:

$$v = At - B/t \tag{2}$$

where A and B are viscometer constants of redistilled water and ethanol (HPLC grade), and t is presented flow time.

The viscosity (η) of the binary solution could be calculated via Eq. [3]

$$\eta = \rho v \tag{3}$$

In order to confirm the repeatability of the data, the experimental values of the density and the viscosity were further compared with literature values and listed in Table 2.

2.2.4. Surface tension of the alcohol-amine binary solutions

Surface tension of the binary solutions was measured with a surface tension meter (BZY-2, Shanghai Balance Instrument). Double-distilled water was used to calibration Wilhelmy plate of the meter before the measurement. All solutions of the surface tension were measured at least three times, and average of three approximate numbers with deviation of ±0.050 $mN \cdot m^{-1}$ were taken to compute final surface tension of the binary solution. Likewise, the experimental and literature values of surface tension of the binary solutions were listed in Table 3.

2.2.5. Spectral characterizations of the alcohol-amine binary solution

UV–Vis of the binary solution wave length was acquired using UV-3200 (Shimadzu) in the range of 190 nm to 400 nm with distinguishability of 1 nm. The wave length of Nicolet (Nexus 670) FTIR spectrometer was 4000–400 cm^{-1} and the spectrometer was set at 1 cm^{-1} distinguishability. Coating solution on circular KBr sheet for measurement. Fluorescence spectra of the binary solution was measured by spectrofluorophotometer-RF-5301pc (Shimadzu), the excitation wavelength of measurement rang were set from 200 nm to 800 nm.

2.2.6. CO_2SM production from alcohol-amine binary solutions

The CO_2SM was prepared as follows: TEG and DAP were mixed at a molar ratio of 1: 1, then CO_2 (99.999 vol%) was pumped into the solution. Weight changes of binary solution were measured every 3 min as CO_2 was absorbing, until the solution completely transformed into a powdery solid and the weight of the binary solution maintain constant.

2.2.7. PHA production using CO_2SM

Growing condition for cyanobacterium CO_2 that captured in the CO_2SM was further used as potential carbon source for PHA (bioplastic) production by an alkalophilic cyanobacterium isolated from a local saline soda lake, Hohhot, China. BG11 medium was used as basal medium for culturing cyanobacterium. The components of the medium are as follows (per liter): 1.5 g of $NaNO_3$, 0.04 g of K_2HPO_4, 0.075 g of $MgSO_4 \cdot 7H_2O$, 0.036 g of $CaCl_2 \cdot 2H_2O$, 0.02 g of Na_2CO_3, 0.006 g of citric acid, 0.006 g of ammonium ferric citrate, 0.001 g of EDTA-Na, 1 mL of

Table 1
Specification of chemical reagent.

Chemical	Source[b]	Mass fraction purity[b]	Molecular formula
Triethylene glycol	Shanghai Macklin Biochemical Co., Ltd	99.5%	$C_6H_{14}O_4$
1,2-diaminopropane[c]	Shanghai Macklin Biochemical Co., Ltd	99%	$C_3H_{10}N_2$
Ethanol[a]	Tianjin guangfu Technology Development Co. Ltd., China	≥99.8%	C_2H_6O

[a] Chromatographic grade.
[b] Declared by the supplier.
[c] Molecular sieve type 4A.

Table 2
Comparison of experiment density (ρ) and viscosity (η) values of TEG and DAP with literature values at different temperature.

T/K	1,2-propanediamine				TEG			
	ρ/(g·cm^{-3})		η/(mPa·s)		ρ/(g·cm^{-3})		η/(mPa·s)	
	Exp.	Lit.	Exp.	Lit.	Exp.	Lit.	Exp.	Lit.
	0.8637	0.8633[17]	1.64	1,62[17]	1.1235	1.1237 [21]	47.6	48.1 [19]
293.15						1.1239 [18]		
	0.8587	0.8585[16]	1.48	1.48[16]	1.1195	1.1198 [21]	37.4	37.1 [23]
298.15		0.8583[17]		1.46[17]		1.1197 [22]		37.1 [18]
	0.8537	0.8538[16]	1.29	1.31[16]	1.1157	1.1159 [21]	29.3	29.2 [18]
303.15		0.8540[17]		1.32[17]		1.1164 [23]		29.2 [24]
	0.8487	0.8492[16]	1.18	1.17[16]	1.1118	1.1120 [21]	23.6	23.7 [23]
308.15		0.8496[17]		1.20[17]		1.1122 [23]		23.7 [19]
	0.8446	0.8445[16]	1.05	1.06[16]	1.1080	1.1081 [20]	19.1	19.2 [23]
313.15		0.8442[17]		1.08[17]		1.1080 [21]		18.3 [20]
	0.8412	0.8399[16]	0.99	0.96[16]	1.1042	1.1046 [23]	16.6	16.1[18]
318.15		0.8413[17]		0.96[17]		1.1042 [20]		

The uncertainties are $u(T) = \pm 0.01$ K, $u(x_1) = \pm 0.0001$ for the density (ρ), the uncertainties are $u(T) = \pm 0.01$ K, $u(t) = \pm 0.01$ s and $u(x_1) = \pm 0.0001$ for the viscosity (η); $U(\rho) = \pm 0.02$ g·cm^{-3}; $U(\eta) = \pm 0.028$ mPa·s (level of confidence = 0.95).

trace element solution. Each liter of the trace element solution contains: 2.86 mg of H_3BO_3, 1.81 mg of $MnCl_2 \cdot 4H_2O$, 0.222 mg of $ZnSO_4 \cdot 7H_2O$, 0.39 mg of $NaMoO_4 \cdot 2H_2O$, 0.079 mg of $CuSO_4 \cdot 5H_2O$, 0.0494 mg of Co $(NO_3)_2 \cdot 6H_2O$. The following groups were compared for PHA production: (i) The BG11 medium was used as control. (ii) Due to CO_2SM contains nitrogen as form of DAP, we used the CO_2SM with replacement to $NaNO_3$ of BG11 medium while maintaining the same nitrogen concentration in the medium (that is 1.5 g of CO_2SM per liter of medium) 10 v/v% 24 h-old pre-grown cells culture was inoculated under above conditions in a 500 mL bubbled flask with 300 mL growing volume. The culture was grown under the continuous lighting condition (338 lx during the daytime and 52 lx during the nighttime) for 12 days. The air flow into the culture was set at 7.2 L/min. Biomass were collected after 12 days for PHA analysis. Three biological replications were conducted when calculating the PHA production from cyanobacterium.

PHA analysis: Intracellular PHA content was analyzed by a Gas Chromatography (GC2014C) via internal standard method [26], briefly, about 10 mg of dry cell biomass was weighted out via scale (Sartorius BS224S) and subjected for methylation. 2 mL chloroform, 2 mL the binary solution of concentrated sulfuric acid (15%) and methanol (85%) was added into the mixture and 2 mg of benzoic acid was added as an internal standard. Esterification was carried out at 98 °C about 4 h, 1 mL distilled water was added when the solution was cooled, and 1 μL of the organic layer was taken for GC (GC2014C Shimadzu) analysis running at following program: initial temperature at 75 °C maintain 4 min, form 75 °C to 250 °C with increasing of 20 °C/min, and final temperature at 250 °C maintain 4 min. PHA production in the sample was identified using PHB standard sample, and confirm via GC–MS (7890B-7000D Agilent), the analysis running at following program: initial temperature at 50 °C, from 50 °C to 180 °C with increasing of 10 °C/min.

Table 3
Comparison of experiment surface tension (γ) values of TEG and DAP with literature values at different temperature.

T/K	TEG	
	γ/(mN·m^{-1})	
	Exp.	Lit.
298.15 K	45.2866	45.67 [25]
303.15 K	45.0533	45.02 [25]
313.15 K	44.2966	43.93 [25]

The uncertainties are $u(T) = \pm 0.01$ K, and $u(x_1) = \pm 0.0001$ for the surface tension; $U(\gamma) = \pm 0.020$ mN·m^{-1}. (level of confidence = 0.95).

3. Results and discussion

3.1. Basic properties of DAP and TEG binary solution

3.1.1. Density

The density of the alcohol-amine binary solution with different mole fractions of two chemicals was measured under six temperature and 88.94 kPa, and the results were shown in Table 4 and Fig. 1. It can be seen from Fig. 1 that under the constant temperature, the density of different binary solutions increased with the increase of TEG mole fractions. Under a certain mole fraction, the density of the binary solution decreased with the increasing temperature.

The relationship between density and composition of binary solution was shown in Eq. (4), and the relationship between density and temperature was shown in Eq. (5) [27,28]

$$\rho_{cal1} = \sum_{i=0}^{4} a_i x_1^i \tag{4}$$

$$\rho_{cal2} = b_0 + b_1 T + b_2 T^2 \tag{5}$$

where a_i, b_0, b_1, b_2 represent the undetermined factor. ρ_{cal1} and ρ_{cal2} represent the calculated values of density. x_1^i represents the molar component of TEG.

The average deviation of density was calculated in Eq. (6) [29].

$$\mathrm{AAD}\% = \frac{\sum \left[100 \times \frac{\rho_{exp} - \rho_{cal}}{\rho_{exp}} \right]}{n} \tag{6}$$

where ρ_{exp} represents the density measured experimentally. n represents the number of experiments.

The density deviation between the experimental values and the calculated values was shown in Figs. S1 and S2, Tables S1 and S2 showed the fitting parameters, average deviation and the fitting degree of density with mole fraction of TEG and temperature.

The excess molar volume (V_m^E) of the binary solution were calculated by experiment density values as Eq. (7) [30].

$$V_m^E = \frac{x_1 M_1 + x_2 M_2}{\rho} - \left(\frac{x_1 M_1}{\rho_1} + \frac{x_2 M_2}{\rho_2} \right) \tag{7}$$

ρ, ρ_1, ρ_2 represent the density of the binary mixture, pure TEG and pure DAP severally. x_1, x_2 and M_1, M_2 represent the relative molar fractions and mole mass of pure TEG and DAP. The result of excess molar volume was listed at Table 5 and Fig. 2.

Table 4
Experimental density (ρ) values of TEG [1] + DAP [2] at $T = 293.15$ K–318.15 K and the pressure of measurement at 88.94 kPa.

x_1	$\rho/(g\cdot cm^{-3})$					
	293.15 K	298.15 K	303.15 K	308.15 K	313.15 K	318.15 K
0.0000	0.8637	0.8587	0.8537	0.8487	0.8446	0.8412
0.0253	0.8768	0.8719	0.8672	0.8621	0.8573	0.8523
0.0520	0.8885	0.8839	0.8791	0.8743	0.8697	0.8649
0.0801	0.9008	0.8960	0.8912	0.8866	0.8819	0.8772
0.1098	0.9138	0.9091	0.9044	0.8996	0.8949	0.8899
0.1413	0.9261	0.9215	0.9169	0.9122	0.9075	0.9027
0.1746	0.9392	0.9346	0.9301	0.9255	0.9208	0.9158
0.2100	0.9528	0.9481	0.9438	0.9389	0.9341	0.9295
0.2476	0.9663	0.9619	0.9573	0.9525	0.9479	0.9433
0.2877	0.9811	0.9767	0.9720	0.9673	0.9625	0.9576
0.3305	0.9951	0.9905	0.9858	0.9811	0.9766	0.9717
0.3763	1.0090	1.0044	1.0000	0.9953	0.9908	0.9860
0.4254	1.0227	1.0183	1.0137	1.0093	1.0046	0.9999
0.4783	1.0361	1.0317	1.0273	1.0232	1.0190	1.0145
0.5352	1.0501	1.0459	1.0414	1.0370	1.0326	1.0279
0.5969	1.0631	1.0591	1.0546	1.0503	1.0460	1.0415
0.6638	1.0757	1.0719	1.0675	1.0631	1.0589	1.0547
0.7366	1.0881	1.0842	1.0800	1.0757	1.0718	1.0675
0.8162	1.1002	1.0962	1.0922	1.0882	1.0840	1.0800
0.9036	1.1119	1.1081	1.1040	1.1001	1.0963	1.0924
1.0000	1.1235	1.1195	1.1157	1.1118	1.1080	1.1042

The standard uncertainty components u for each variables are $u(T) = \pm 0.01$ K, $u(x_1) = \pm 0.0001$, the combined expanded uncertainty is $U(\rho) = \pm 0.02$ g·cm^{-3} at 0.95 confidence level.

Fig. 2 showed that the excess molar volumes of the binary solution were all negative, which was due to the negative deviation from additively behavior [31]. The binary system showed a strong affinity between two molecules, when the interval of two molecules decreased and volume of the solution shrinkage [27]. When the molar ratio of the two molecules (TEG and DAP) in binary solution was 1: 1, the maximum interaction between the molecules has occurred. [32]. Physical interaction also plays an important role in the binary solution. With the increased temperature, the excess molar volumes of the binary solution first decreased and then increased suggesting the temperature was conducive to molecular interactions [32].

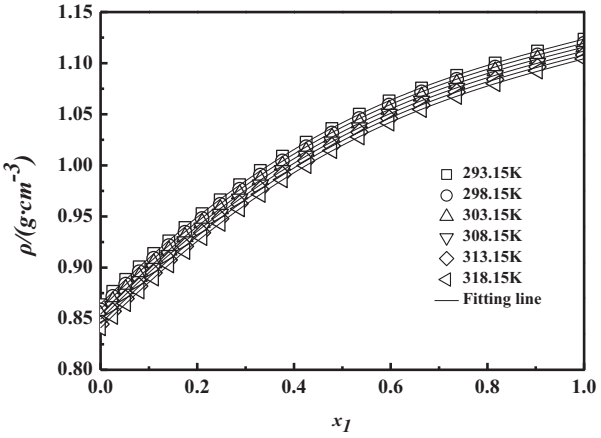

Fig. 1. Experimental density values with mole fraction for TEG [1] + DAP [2] binary solution at $T = 293.15$ K–318.15 K: □ 293.15 K; ○ 298.15 K; △ 303.15 K; ▽ 308.15 K; ◇ 313.15 K; ◁318.15 K.

The V_{mcal}^{E} was fitted in the form of Redlich-Kister Eq. (8) [33].

$$Y = x_1(1-x_1)\sum_{i=0}^{n} A_i(2x_1-1)^i \tag{8}$$

where Y is V_{mcal}^{E} or $\Delta\eta_{cal}$, A_i represent fitting parameters, and n is number of polynomials. Factors of Redlich-Kister equation and standard deviation for V_{mcal}^{E} of TEG [1] + DAP [2] at 293.15 K - 318.15 K listed in Table S3.

In order to research the fitting degree of V_m^E, $\Delta\eta$ and $\Delta\gamma$, the standard deviation of experimental and calculated values was calculated by Eq. (9) [9].

$$\sigma = \left[\sum_{i=1}^{n}\left(V_{exp.i}^{E} - V_{cal.i}^{E}\right)^2/(N-n)\right]^{\frac{1}{2}} \tag{9}$$

Table 5
Excess molar volume (V_m^E) for TEG [1] + DAP [2] binary mixture at T = (293.15 to 318.15) K with the step of 5 K.

x_1	$V_m^E/(cm^3 \cdot mol^{-1})$					
	T = 293.15 K	T = 298.15 K	T = 303.15 K	T = 308.15 K	T = 313.15 K	T = 318.15 K
0.0000	0.0000	0.0000	0.0000	0.0000	0.0000	0.0000
0.0253	−0.2987	−0.3102	−0.3353	−0.3265	−0.2677	−0.1059
0.0520	−0.4362	−0.4687	−0.4969	−0.5139	−0.4720	−0.3313
0.0801	−0.6051	−0.6279	−0.6480	−0.6824	−0.6362	−0.5109
0.1098	−0.8216	−0.8534	−0.8803	−0.8968	−0.8484	−0.6946
0.1413	−0.9426	−0.9823	−1.0122	−1.0451	−1.0017	−0.8724
0.1746	−1.1190	−1.1488	−1.1930	−1.2306	−1.1836	−1.0411
0.2100	−1.3114	−1.3341	−1.3971	−1.3998	−1.3470	−1.2453
0.2476	−1.4794	−1.5232	−1.5531	−1.5651	−1.5342	−1.4343
0.2877	−1.7375	−1.7834	−1.7999	−1.8252	−1.7692	−1.6459
0.3305	−1.8947	−1.9118	−1.9235	−1.9439	−1.9218	−1.7982
0.3763	−2.0003	−2.0258	−2.0593	−2.0774	−2.0532	−1.9436
0.4254	−2.0648	−2.1000	−2.1149	−2.1436	−2.0976	−2.0030
0.4783	−2.0630	−2.0884	−2.1137	−2.1711	−2.1763	−2.1041
0.5352	−2.0821	−2.1227	−2.1366	−2.1526	−2.1357	−2.0359
0.5969	−1.9595	−2.0186	−2.0166	−2.0313	−2.0151	−1.9468
0.6638	−1.7466	−1.8160	−1.8126	−1.8172	−1.8009	−1.7665
0.7366	−1.4650	−1.5080	−1.5119	−1.5150	−1.5261	−1.4740
0.8162	−1.0833	−1.1122	−1.1191	−1.1362	−1.1088	−1.0909
0.9036	−0.5923	−0.6211	−0.6089	−0.6194	−0.6304	−0.6250
1.0000	0.0000	0.0000	0.0000	0.0000	0.0000	0.0000

N is based on experimental points and n is the number of factors.

The apparent molar volume of TEG [1] + DAP [2] were obtained from Eqs. (10) and (11), and the experimental values were shown in Table S4 [34].

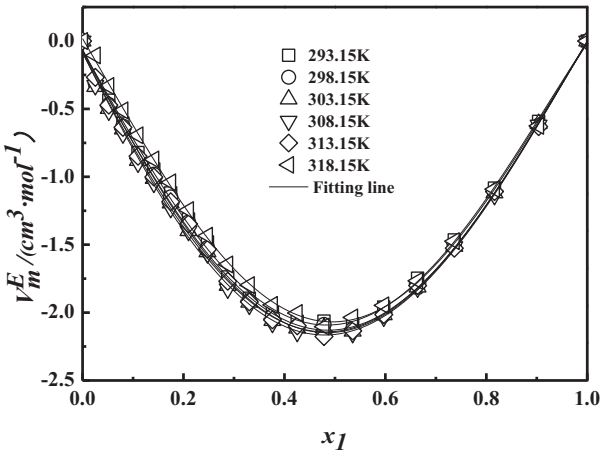

Fig. 2. Excess molar volumes with mole fraction for TEG [1] + DAP at T = 293.15 K–318.15 K: □ 293.15 K; ○ 298.15 K; △ 303.15 K; ▽ 308.15 K; ◇ 313.15 K; ◁ 318.15 K.

$$V_{\varphi,1} = \frac{x_2 M_2}{x_1} \times (\rho_2 - \rho)/\rho_2 \rho + M_1/\rho \tag{10}$$

$$V_{\varphi,2} = \frac{x_{1M_1}}{x_2} \times (\rho_1 - \rho)/\rho_1 \rho + M_2/\rho \tag{11}$$

where ρ_1, ρ_2, are the density values of pure TEG and pure DAP and M_1, M_2 represent the molecular mass of pure TEG and pure DAP. ρ is the density of binary solution.

Partial molar volume of the binary solution was calculated by Eqs. (12) and (13) [28]:

$$\overline{V}_1 = V_m^E + V_1^0 + (1 - x_1)\left(\frac{\partial V_m^E}{\partial x_1}\right)_{P,T} \tag{12}$$

$$\overline{V}_2 = V_m^E + V_2^0 - x_1\left(\frac{\partial V_m^E}{\partial x_1}\right)_{P,T} \tag{13}$$

where V_1^0 and V_2^0 are the molar volume of pure component and the datum was listed in Table S5.

Accord to the Table S4, under the certain temperature, the apparent molar volumes of binary solution $V_{\varphi,1}$ and $V_{\varphi,2}$ decreased with increase

of mole fraction of TEG. At a certain mole fraction of TEG, the apparent molar volumes of binary solution $V_{\varphi,1}$ increased along with increasing temperature. When the mole fraction of TEG x_1 at 0–0.4738, the apparent molar volumes of binary solution $V_{\varphi,2}$ increased, when the mole fraction of TEG x_1 at 0.5353–0.9036, the apparent molar volumes of binary solution $V_{\varphi,2}$ decreased with increasing temperature. Table S5 showed that partial molar volume of the binary solution $\overline{V}_1$ increased and $\overline{V}_2$ first decreased then increased with the increasing mole fraction of TEG At a certain mole fraction of TEG, the partial molar volume $\overline{V}_1$ and $\overline{V}_2$ increased with increasing temperature.

3.1.2. Viscosity

The viscosity datum of TEG [1] + DAP [2] binary solution were shown in Table 6, and the fitting figure of viscosity was depicted in Fig. 3.

As shown in the Fig. 3 and Table 6, under the same temperature, the viscosity of the binary solution increased first and then decreased with the increasing mole fraction of TEG. Within the temperature of 293.15 K - 303.15 K, when the mole fraction of TEG at $x_1 \approx 0.6638$, the solution reached at the maximum of viscosity. Within the temperature of 308.15 K - 318.15 K, when the mole fraction of TEG at $x_1 \approx 0.7366$, viscosity of the binary solution reached at the maximum

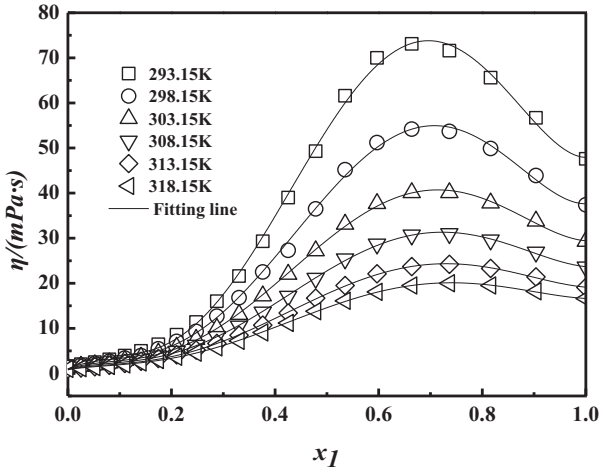

Fig. 3. Experimental viscosity values with mole fraction for TEG [1] + DAP [2] binary solution at $T = 293.15$ K–318.15 K: □ 293.15 K; ○ 298.15 K; △ 303.15 K; ▽ 308.15 K; ◇ 313.15 K; ◁318.15 K.

Table 6
Experimental viscosity (η) values of TEG [1] + DAP [2] at T = 293.15 K–318.15 K and the pressure of measurement at 88.94 kPa.

x_1	η/(mPa·s)					
	293.15 K	298.15 K	303.15 K	308.15 K	313.15 K	318.15 K
0.0000	1.64	1.48	1.29	1.18	1.05	0.99
0.0253	2.04	1.82	1.59	1.41	1.26	1.17
0.0520	2.50	2.20	1.92	1.70	1.50	1.39
0.0801	3.11	2.71	2.34	2.05	1.81	1.66
0.1098	3.96	3.41	2.91	2.52	2.20	2.00
0.1413	5.00	3.96	3.60	3.10	2.68	2.43
0.1746	6.47	5.45	4.53	3.87	3.30	2.97
0.2100	8.59	7.11	5.82	4.90	4.13	3.69
0.2476	11.5	9.32	7.57	6.24	5.19	4.59
0.2877	16.0	12.7	10.0	8.18	6.64	5.78
0.3305	21.6	16.8	13.1	10.5	8.46	7.22
0.3763	29.3	22.5	17.2	13.6	10.7	9.08
0.4254	39.0	27.4	22.0	17.1	13.4	11.2
0.4783	49.3	36.5	27.2	21.1	16.7	13.8
0.5352	61.7	45.2	33.1	25.4	19.5	16.1
0.5969	70.0	51.2	37.7	28.7	22.1	18.1
0.6638	73.1	54.2	40.1	30.7	23.7	19.5
0.7366	71.6	53.7	40.1	31.0	24.2	20.0
0.8162	65.6	49.9	37.8	29.6	23.3	19.5
0.9036	56.7	43.9	33.8	26.9	21.4	18.2
1.0000	47.6	37.4	29.3	23.6	19.1	16.6

The standard uncertainty components u for each variables are $u(x_1) = \pm 0.0001$, $u(T) = \pm 0.01$ K, $u(t) = \pm 0.01$ s, the relative expanded uncertainty is $U(\eta) = \pm 0.028$ mPa·s at 0.95 confidence level.

values. Under the constant mole fraction of TEG, viscosity of the binary solution decreased with the increasing temperature. This phenomenon indicated that when the system temperature increased, the molecular energy of the binary solution tends to increase, and inter molecular flows of two chemicals increased, therefore the overall viscosity of the solution decreased [35].

The viscosity (η) values of the binary solution were calculated by Eqs. (14) and (15) [36].

$$\eta_{cal.1} = \sum_{j=0}^{6} c_j x_1^i \tag{14}$$

$$\eta_{cal.2} = \eta_0 \exp\left(\frac{Ea}{RT}\right) \tag{15}$$

where c_j, η_0 are an undetermined factors, **R is** perfect gas constant, and Ea is activity energy. $\eta_{cal.1}$ and $\eta_{cal.2}$ were computed by Eqs. (14) and (15). The results of the binary solution viscosity deviation between the experimental values and the calculated values were showed in Figs. S3 and S4. Undetermined coefficient, AAD% and R-Squared were listed in Tables S6 and S7.

The equation of viscosity deviation is as Eq. (16) [37]:

$$\Delta\eta = \eta - x_1\eta_1 - x_2\eta_2 \tag{16}$$

where η_1, η_2, η are the viscosity of the two pure components solution and the mixed component solution. The viscosity deviation results and the corresponding fitting diagram was shown in Table 7 and Fig. 4. Factors of Redlich-Kister equation and standard deviation of TEG [1] + DAP [2] at 293.15 K - 318.15 K derived from viscosity deviation values were displayed in Table S8.

According to Fig. 4, under different experimental temperature, the changes in viscosity deviation of binary solution followed the same trend, with a slight rise at the mole fraction of TEG $x_1 \approx 0$–0.2476 and then decreased at the mole fraction of TEG $x_1 \approx 0.2877$–1. When the temperature was constant, the viscosity deviation of binary solution first decreased, then increased and decreased again till the end of the experiment. The minimum and the maximum values of viscosity deviation was at $x_1 \approx 0.1413$, and $x_1 \approx 0.6638$.

3.1.3. Surface tension

Surface tension was a significant physical property to indicate the interaction of mixed solution, both long-distance attraction and short-distance repulsion of liquid have effects on surface tension of the mixed solution. On the surface of solution, these forces are not balanced so that the surface of solution exhibits a storage attraction [25].

Surface tension data of TEG [1] + DAP [2] at 293.15 K - 318.15 K were listed in Table 8 and depicted in Fig. 5.

According to Fig. 5, the changes in surface tension of binary solution under the different experimental temperature followed the same trend, with a rapid rose by an increased TEG mole fraction, and gradually

Table 7
Viscosity deviation ($\Delta\eta$) for TEG [1] + DAP [2] binary mixture at T = (293.15 to 318.15) K with the step of 5 K.

x_1	$\Delta\eta$/(mPa·s)					
	293.15 K	298.15 K	303.15 K	308.15 K	313.15 K	318.15 K
0.0000	0.000	0.000	0.000	0.000	0.000	0.000
0.0253	−0.760	−0.575	−0.412	−0.333	−0.249	−0.217
0.0520	−1.52	−1.14	−0.829	−0.643	−0.485	−0.414
0.0801	−2.21	−1.65	−1.20	−0.921	−0.689	−0.581
0.1098	−2.73	−2.02	−1.46	−1.11	−0.833	−0.698
0.1413	−3.13	−2.59	−1.65	−1.24	−0.922	−0.759
0.1746	−3.20	−2.30	−1.65	−1.21	−0.902	−0.736
0.2100	−2.70	−1.92	−1.35	−0.976	−0.702	−0.568
0.2476	−1.57	−1.05	−0.652	−0.482	−0.329	−0.258
0.2877	1.14	0.861	0.695	0.567	0.402	0.314
0.3305	4.77	3.43	2.53	1.93	1.45	1.09
0.3763	10.4	7.47	5.38	3.97	2.91	2.23
0.4254	17.8	10.6	8.81	6.42	4.69	3.62
0.4783	25.7	17.9	12.5	9.18	7.05	5.34
0.5352	35.4	24.5	16.9	12.2	8.79	6.73
0.5969	40.9	28.3	19.7	14.2	10.3	7.86
0.6638	40.9	28.9	20.2	14.7	10.7	8.19
0.7366	36.1	25.8	18.2	13.3	9.82	7.52
0.8162	26.4	19.1	13.6	10.1	7.50	5.77
0.9036	13.5	9.98	7.27	5.50	4.09	3.14
1.0000	0.000	0.000	0.000	0.000	0.000	0.000

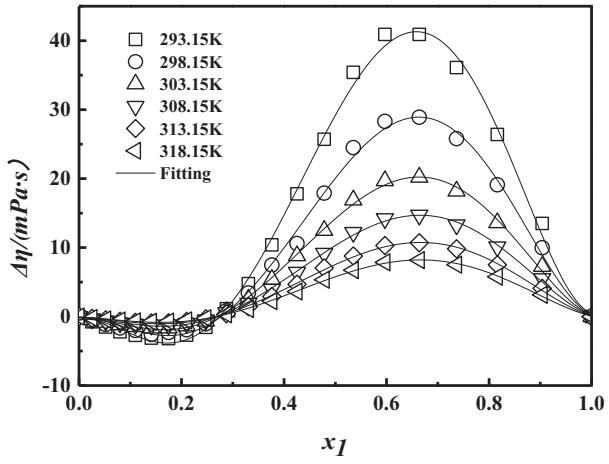

Fig. 4. Viscosity deviation for TEG [1] + DAP [2] binary mixture at $T = (293.15$ to $318.15)$ K with the step of 5 K. □ 293.15 K; ○ 298.15 K; △ 303.15 K; ▽ 308.15 K; ◇ 313.15 K; ◁318.15 K.

plateaued with further elevated TEG concentration. Higher surface tension of TEG than DAP is likely the primary reason for observed changes. Furthermore, when the mole fraction of solution was constant, the surface tension of the binary solution decreased with the increasing temperature. This may due to the intermolecular attraction between TEG and DAP decreased with increasing temperature.

The surface tension (γ) values were calculated by Eqs. (17) and (18) [38]. The deviation between the calculated and experimental values of the surface tension was shown in Figs. S5 and S6.

$$\gamma_{cal.1} = d_4x_1^4 + d_3x_1^3 + d_2x_1^2 + d_1x_1 + d_0 \tag{17}$$

$$\gamma_{cal.2} = e_1T + e_0 \tag{18}$$

where d_5, d_4, d_3, d_2, d_1, d_0, e_1, and e_0 represent undetermined parameters. Tables S9 and S10 showed the fitting parameters, average deviation and the fitting degree of surface tension with mole fraction of TEG and temperature.

The surface tension deviation value of TEG [1] + DAP was calculated by Eq. (19) [39]:

$$\Delta\gamma = \gamma - \sum_{i=1}^{2} x_i y_i \tag{19}$$

x_i, γ_i represent molar composition and surface tension of solution.

Table 8
Experimental surface tension (γ) values of TEG [1] + DAP [2] at $T = 293.15$ K–318.15 K and the pressure of measurement at 88.94 kPa.

x_1	$\gamma/(\mathrm{mN\cdot m^{-1}})$					
	T = 293.15 K	*T = 298.15 K*	*T = 303.15 K*	*T = 308.15 K*	*T = 313.15 K*	*T = 318.15 K*
0.0000	33.70	33.14	32.81	32.37	31.89	31.46
0.0253	34.02	33.26	33.23	32.93	32.28	31.88
0.0520	34.36	33.77	33.54	33.21	32.65	32.25
0.0801	34.83	34.50	34.23	33.63	33.21	32.77
0.1098	35.23	34.68	34.50	34.13	33.71	33.23
0.1413	35.81	35.33	35.06	34.56	34.38	33.82
0.1746	36.37	35.76	35.73	35.18	34.88	34.55
0.2100	36.99	36.45	36.18	35.87	35.54	35.15
0.2476	37.70	37.27	37.01	36.78	36.31	36.01
0.2877	38.60	37.94	37.72	37.30	36.92	36.52
0.3305	39.29	38.73	38.59	38.11	37.90	37.32
0.3763	40.15	39.55	39.41	39.15	38.80	38.47
0.4254	41.07	40.34	40.17	39.74	39.67	39.30
0.4783	41.69	41.07	40.92	40.81	40.37	40.07
0.5353	42.63	41.84	41.63	41.70	41.29	40.94
0.5969	43.40	42.69	42.42	42.13	41.83	41.48
0.6638	43.84	43.24	43.14	42.81	42.32	42.17
0.7366	44.41	43.89	43.82	43.51	43.11	42.73
0.8163	44.93	44.52	44.26	44.14	43.70	43.27
0.9036	45.42	44.64	44.56	44.54	44.05	43.58
1.0000	45.80	45.53	45.05	44.55	44.30	43.99

The standard uncertainty components u for each variables are $u(T) = \pm 0.01$ K and $u(x_1) = \pm 0.0001$, the relative expanded uncertainty is $U(\gamma) = \pm 0.020\ \mathrm{mN\cdot m^{-1}}$ at 0.95 confidence level.

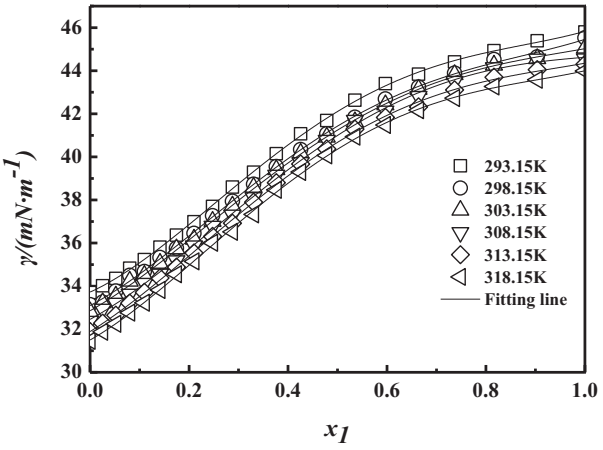

Fig. 5. Experimental surface tension with mole fraction for TEG [1] + DAP [2] binary solution at $T = 293.15$ K–318.15 K: □ 293.15 K; ○ 298.15 K; △ 303.15 K; ▽ 308.15 K; ◇ 313.15 K; ◁318.15 K.

The resulting surface tension deviation data were displayed in Table 9 and Fig. 6.

According to Fig. 6, the surface tension deviation ($\Delta\gamma$) of solution under the same temperature increased at first and then decreased with the increase of TEG mole fraction. When the temperature at 293.15–303.15 K, the surface tension deviation reached the maximum value at $x_1 \approx 0.59$. When the temperature at 308.15–318.15 K, the surface tension deviation reached the maximum value at $x_1 \approx 0.53$.

The $\Delta\gamma_{cal}$ was fitted in the form of Redlich-Kister Eq. [20] [40].

$$\Delta\gamma_{cal} = x_1(1-x_1)\sum_{i=0}^{n} E_i(2x_1-1)^i \quad (20)$$

where E_i represent fitting parameters, n is number of polynomials. Factor of Redlich-Kister equation and standard deviation of TEG [1] + DAP [2] at 293.15 K - 318.15 K listed in Table S11.

3.1.4. Spectral properties

The UV spectra results of TEG [1] + DAP [2] binary solution with different mole faction of the two molecules was shown in Fig. 7. With the increasing amount of DAP, the ultraviolet absorption has a red shift with the wavelength shift from 201 nm to 206 nm. This phenomenon was due to the n-σ* electron transition of lone electron pairs of oxygen atoms of hydroxyl groups in TEG. The addition of amines breaks the intermolecular force of TEG, subsequently the interaction between the TEG and the DAP was formed [40].

Fig. 8 showed the FTIR spectral results of pure TEG, pure DAP, and TEG [1] + DAP [2] binary solution with different mole fraction of two components. A storage and wide peak between 3450 cm^{-1} -

Table 9
Surface tension deviation ($\Delta\gamma$) for TEG [1] + DAP [2] binary mixture at T = (293.15 to 318.15) K with the step of 5 K.

x_1	$\Delta\gamma$(mN·m^{-1})					
	293.15 K	298.15 K	303.15 K	308.15 K	313.15 K	318.15 K
0.0000	0.00	0.00	0.00	0.00	0.00	0.00
0.0253	0.01	−0.19	0.12	0.25	0.08	0.10
0.0520	0.02	−0.01	0.10	0.21	0.12	0.14
0.0801	0.15	0.36	0.44	0.28	0.33	0.31
0.1098	0.20	0.17	0.35	0.43	0.46	0.39
0.1413	0.39	0.44	0.53	0.48	0.74	0.59
0.1746	0.56	0.45	0.79	0.69	0.82	0.90
0.2100	0.75	0.70	0.81	0.95	1.05	1.06
0.2476	1.00	1.06	1.17	1.40	1.35	1.44
0.2877	1.41	1.23	1.39	1.43	1.46	1.45
0.3305	1.59	1.50	1.74	1.72	1.91	1.73
0.3763	1.90	1.74	2.00	2.20	2.25	2.29
0.4254	2.22	1.93	2.16	2.19	2.50	2.51
0.4783	2.20	2.00	2.26	2.62	2.55	2.61
0.5353	2.45	2.06	2.27	2.82	2.76	2.77
0.5969	2.48	2.16	2.31	2.49	2.54	2.54
0.6638	2.11	1.88	2.20	2.35	2.20	2.39
0.7366	1.80	1.62	1.99	2.17	2.08	2.03
0.8163	1.35	1.27	1.45	1.83	1.68	1.58
0.9036	0.79	0.30	0.69	1.16	0.95	0.79
1.0000	0.00	0.00	0.00	0.00	0.00	0.00

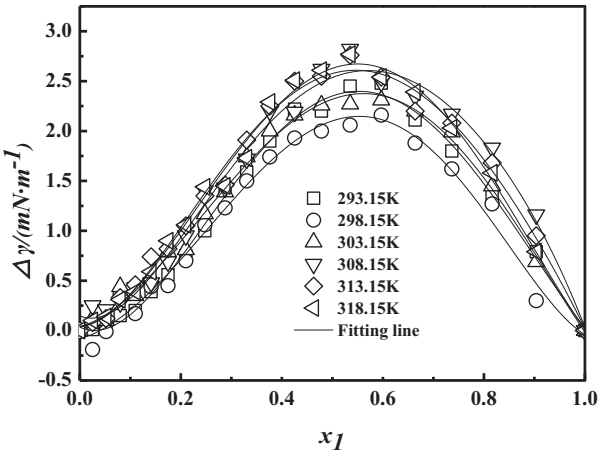

Fig. 6. Surface tension deviation for TEG [1] + DAP [2] binary mixture at $T = (293.15$ to 318.15) K with the step of 5 K. □ 293.15 K; ○ 298.15 K; △ 303.15 K; ▽308.15 K; ◇ 313.15 K; ◁318.15 K.

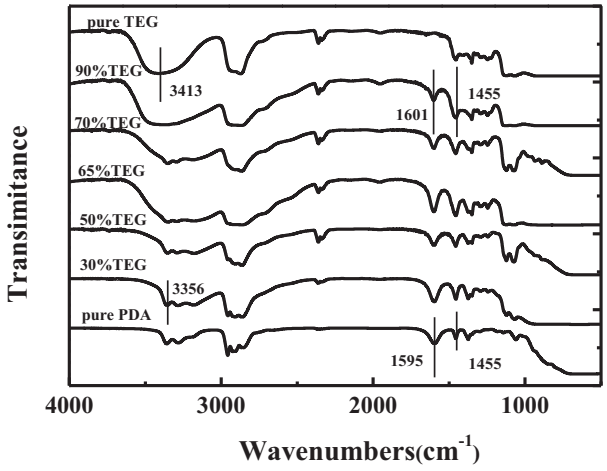

Fig. 8. FTIR spectra for TEG [1] + DAP binary solution, mole percentage of TEG respectively 100%, 90%, 70%, 65%, 50%, 30% and 0%.

3200 cm^{-1} presented the hydroxide radical. A stretching vibration peak was found at 3413 cm^{-1}, which belongs to the stretching vibration peak of hydroxide radical of pure TEG according to pervious work by Hao and Qiao [18,23]. By adding DAP, the peak of hydroxide radical moved toward lower wave range at 3356 cm^{-1}, meanwhile the alcoholic hydroxyl spectrum was narrowed, this may due to intermolecular force reduced the average density of the electron cloud and the bond force constant between two molecules [41]. The -NH stretching vibration peak of -NH_2 was identified at 1595 cm^{-1}, and it was found that with increasing TEG fraction, the –NH peak moved from 1595 cm^{-1} to 1601 cm^{-1}. Hydrogen bonds between TEG and DAP may exist in the form of O—H, N—O or N—H. The changes of wavelength due to bending vibration of DAP was less than the changes caused by the stretching vibration of hydroxyl-TEG, which can be explained as hydrogen bond self-association of TEG destruction and formation of intermolecular hydrogen bonds between H-TEG and N-DAP as addition of DAP [40,7].

Fig. 9 depicted the fluorescence spectra of pure TEG and the binary solution of TEG [1] + DAP [2]. The lone electron pair of hydroxyl oxygen in pure TEG has a n-electronic transitions near 332 nm. With the increase DAP fraction, the intensity of the absorption peak shifted from 332 nm to 339 nm. The result indicated that the oxygen in the –OH group returned to the ground state, the energy released was reduced, the transition of lone electron pairs of oxygen atoms of hydroxyl groups in TEG has occurred. Because of the addition of amines, the hydrogen atom on OH-TEG was attracted by the nitrogen atom in DAP, and new intermolecular force was formed between DAP and TEG [28].

3.2. Preparation of CO_2SM

According to the data of the excess mole volume of the binary solution, when molar ratio of TEG to DAP was 1: 1, intermolecular force between TEG and DAP was stronger, the capacity of CO_2 absorption by the binary solution was tested, and 0.34 g CO_2 was absorbed by per 1 g DAP + TEG. The absorption of CO_2 by the binary solution in this work was less than that of Zhao [40], which could be due mostly to the method of two studies: stirring with the rotor during the CO_2 absorption in this study facilitated the absorption speed while with less efficient absorption potential.

3.3. Production of PHB using CO_2SM

The CO_2SM was then used as the potential carbon source for PHB production by a newly isolated cyanobacterium from local alkane-soda lake. The strain was able to grow under relative high pH at 9, providing adaption to CO_2SM containing medium. PHB production of the strain was identified using a commercial PHB standard by GC, and the candidate peak was further confirmed via GC–MS (the peak identification of PHB by GC–MS was depicted in Fig. S7). The PHB production from CO_2SM

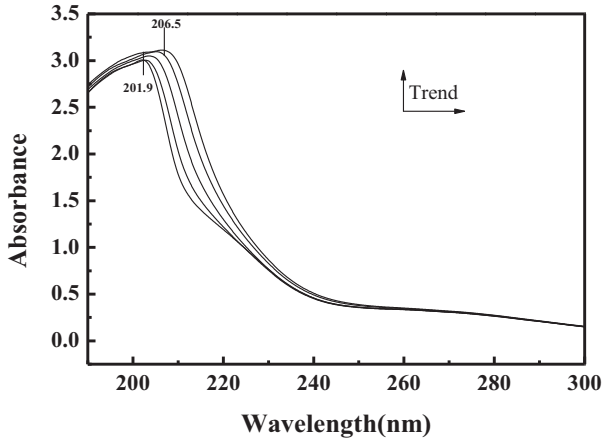

Fig. 7. UV–Vis spectra for TEG [1] + DAP binary solution and electronic transitions redshift from 201.9 to 206.5 nm with the increasing DAP concentration.

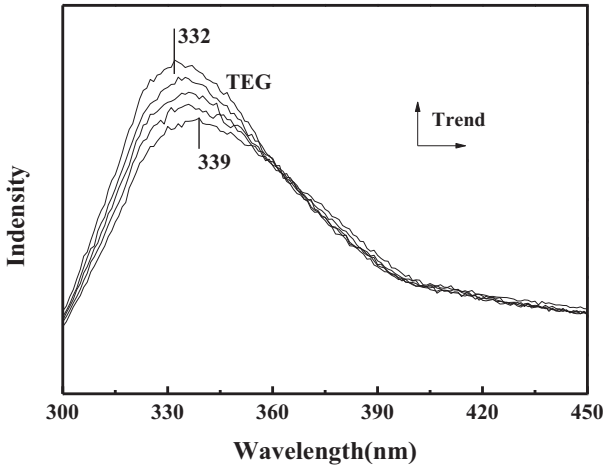

Fig. 9. Fluorescence spectra of TEG [1] + DAP mixtures with various concentration.

containing medium after 10 days of cultivation was at average of 12.92 wt % while only 4.64 wt% from the control group (BG-11 only) (Fig. 10). PHB production from cyanobacterium under autotrophic condition is normally limited to lower mass transfer of actual CO_2 (carbon source) to cyanobacterium cell and non-optimized intracellular carbon/energy distribution toward PHB biosynthesis [15,42]. The alkalinic culturing condition may provide a stable source of carbon in form of HCO_3^- and CO_3^{2-} with potential increased mass transfer of CO_2 to the cell leading to a higher PHB production. Our preliminary result on PHB production using novel CO_2 storing material under autotrophic condition suggested that CO_2SM could be used as potential source for the strain without compromising the growth. Further works on optimization of CO_2SM-integrated PHB production was undertaken in the lab currently.

4. Conclusion

In this work, the basic date of density, viscosity and surface tension of TEG [1] + DAP [2] binary solution were measured at T = (293.15 K–318.15 K) with step of 5 K and 88.94 kPa. The excess molar volume (V_m^E), the apparent molar volume ($V_{\varphi,2}$, $V_{\varphi,1}$), partial molar volume ($\overline{V}_1$, $\overline{V}_2$), viscosity deviation ($\Delta\eta$) and surface tension deviation ($\Delta\gamma$) were calculated by the basic date. According to the values of the excess mole volume, when the molar ratio of the two molecules (TEG and DAP) in binary solution was 1: 1, the stronger intermolecular force was formed. UV–Vis, FTIR, and Fluorescence spectrophotometer results comparing between pure solution and the binary solution suggested that intermolecular hydrogen bonds were formed between H in TEG and N in DAP. These results may shed light in understanding and further optimizing CO_2 absorbing capacity of the binary solution. Under current study condition, about 0.34 g CO_2 was absorbed by 1 g of TEG [1] +DAP [2] binary solution at the molar ratio of TEG to DAP at 1: 1. The resulting CO_2SM showed potential as carbon source for biodegradable plastic production using a novel alkalophilic cyanobacterium. The physical and chemical properties of the material may be determining factor for optimal CO_2 absorption and PHA production potential, which deserves further study.

CRediT authorship contribution statement

Xiaoqian Jia: Investigation, writing-orginal draft. **Shuai Zhang:** Investigation. **Bin Li:** Investigation. **Jinrong Yang:** Investigation. **Jianbin Zhang:** Funding acquisition, project administration, supervistion, and writing-review & editing. **Jilagamazhi Fu:** investigation, supervision, writing-review & editing.

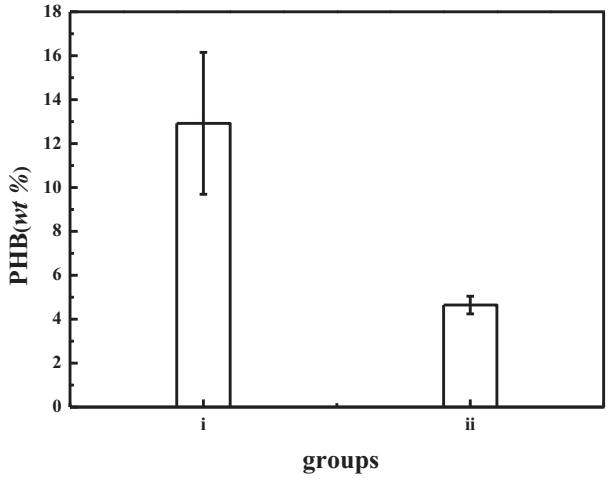

Fig. 10. PHB content of the culture method (i) using BG11 medium, (ii) using storage material instead of sodium nitrate in BG11 medium.

Declaration of competing interest

The authors declare no competing financial interests.

Acknowledgements

This work was supported by the National Natural Science Foundation of China (21666027), the Program for Grassland Excellent Talents of Inner Mongolia Autonomous Region, the Natural Science Foundation of Inner Mongolia Autonomous Region (2016JQ02), the Inner Mongolia Science and Technology Key Projects, and training plan of academic backbone in youth of Inner Mongolia University of Technology.

Appendix A. Supplementary data

Supplementary data to this article can be found online at https://doi.org/10.1016/j.molliq.2020.112804.

References

[1] C. Rosenzweig, D. Karoly, M. Vicarelli, P. Neofoti, Q. Wu, G. Casassa, A. Menzel, T.L. Root, N. Estrella, B. Seguin, P. Tryjanowski, C.Z. Liu, S. Rawlins, A. Imeson, Attributing physical and biological impacts to anthropogenic climate change, Pub. Med. 453 (2008) 353–357.
[2] M. Deanna, D'Alessandro, S. Berend, R.L. Jeffrey, Carbon dioxide capture: prospects for new materials, Angew. Chem. Int. Ed. 49 (2010) 6058–6082.
[3] Z.Y. Fu, Q. Yang, Z. Liu, F. Chen, F.B. Yao, T. Xie, Y. Zhong, D.B. Wang, J. Li, X.M. Li, G.M. Zeng, Photocatalytic conversion of carbon dioxide: from products to design the catalysts, J. CO2 Util. 34 (2019) 63–73.
[4] J. Oexmann, C. Hensel, A. Kather, Post-combustion CO_2-capture from coal-fired power plants: preliminary evaluation of an integrated chemical absorption process with piperazine-promoted potassium carbonate, Int. J. Greenhouse Gas Control. 2 (2008) 539–552.
[5] A. Blanco, A. García-Abuín, D. Gomez-Díaz, J.M. Navaza, Surface tension and refractive index of benzylamine and 1,2-diaminopropane aqueous solutions from T = (283.15 to 323.15) K, J. Chem. Eng. Data 57 (2012) 2437–2441.
[6] R. Idem, M. Wilson, P. Tontiwachwuthikul, A. Chakma, A. Verwab, A. Aroonwilas, D. Gelowitz, Pilot plant studies of the CO_2 capture performance of aqueous MEA and mixed MEA/MDEA solvents at the university of Regina CO_2 capture technology development plant and the boundary dam CO_2 capture demonstration plant, Ind. Eng. Chem. Res. 45 (2006) 2414–2420.
[7] X.L. Meng, X.F. Li, H.H. Shi, J.M. Wu, Z.J. Wu, Density, viscosity and excess properties for binary system of 1.2-ethanediamine + polyethylene glycol 400 at T = (293.15, 298.15, 303.15, 308.15, 313.15, and 318.15) K under atmospheric pressure, J. Mol. Liq. 219 (2016) 677–684.
[8] M. Garcia, H.K. Knuutila, U.E. Aronu, S. Gu, Influence of substitution of water by organic solvents in amine solutions on absorption of CO_2, Int. J. Greenhouse Gas Control 78 (2018) 286–305.
[9] L. Li, J. Zhang, Q. Li, B. Guo, T. Zhao, F. Sha, Density, viscosity, surface tension, and spectroscopic properties for binary system of 1,2-ethanediamine + diethylene glycol, Thermochim. Acta 590 (2014) 91–99.
[10] F. Sha, T. Zhao, B. Guo, X. Ju, L. Li, J. Zhang, Density, viscosity and spectroscopic studies of the binary system 1,2-ethylenediamine + 1,4-butanediol at T = (293.15 to 318.15) K, J. Mol. Liq. 208 (2015) 373–379.
[11] A. Bahadori, H.B. Vuthaluru, S. Mokhatab, Analyzing solubility of acid gas and light alkanes in triethylene glycol, J. Nat. Gas Chem. 17 (2008) 51–58.
[12] J. Tan, H. Shao, J.H. Xu, L. Du, G.H. Luo, Mixture absorption system of monoethanolamine - triethylene glycol for CO_2 capture, Ind. Eng. Chem. Res. 50 (2011) 2437–2441.
[13] L. Zhao, C. Liu, X.Q. Yue, L. Ma, Y. Wu, T.Y. Yang, J.B. Zhang, Application of CO_2 -storage materials as a novel plant growth regulator to promote the growth of four vegetables, J. CO_2 Util. 26 (2018) 537–543.
[14] S.S. Costa, A.L. Miranda, M.G. de Morais, J.A.V. Costa, J.I. Druzian, Microalgae as source of polyhydroxyalkanoates (PHAs) - a review, Int. J. Biol. Macromol. 131 (2019) 536–547.
[15] G.M. Rosa, L. Moraes, M.R.A.Z. Souza, J.A.V. Costa, Spirulina cultivation with a CO_2 absorbent: influence on growth parameters and macromolecule production, Bioresour. Technol. 200 (2016) 528–534.
[16] M.N. Islam, M.A. Ali, M. Monirul Islam, M.K. Nahar, Volumetric and viscometric properties of aqueous solutions of N-methylformamide, 1,2-diaminopropane and 2-methylpropane-2-ol, Phys. Chem. Liq. 41 (2003) 271–282.
[17] R.M. Zhang, X.Q. Yue, B. Li, J.R. Yang, Z.J. Wu, J.B. Zhang, Dynamic viscosity, density and surface tension of 1,3-propanediol (1) + 1,2-propanediamine (2) binary system at T = (293.15 to 318.15) K and atmosphere pressure, J. Mol. Liq. (2020) https://doi.org/10.1016/j.molliq.2019.112213.
[18] C.X. Hao, L. Zhao, X.Q. Yue, Y.J. Pang, J.B. Zhang, Density, dynamic viscosity, excess properties and intermolecular interaction of triethylene glycol + N, N-dimethylformamide binary mixture, J. Mol. Liq. 274 (2019) 730–739.
[19] H.E. Hoga, R.B. Torres, P.L. Onófrio Volpe, Thermodynamics properties of binary mixtures of aqueous solutions of glycols at several temperatures and atmospheric pressure, J. Chem. Thermodyn. 122 (2018) 38–64.

[20] Z.H. Guo, J.B. Zhang, T. Zhang, C.P. Li, Y.F. Zhang, J.B. Liquid viscosities, excess properties, and viscous flow thermodynamics of triethylene glycol + water mixtures at T=(298.15, 303.15, 308.15, 313.15, and 318.15) K, J. Mol. Liq. 165 (2011) 27–31.
[21] A. Valtz, M. Teodorescu, I. Wichterle, D. Richon, Liquid densities and excess molar volumes for water + diethylene glycolamine, and water, methanol, ethanol, 1-propanol + triethylene glycol binary systems at atmospheric pressure and temperatures in the range of 283.15-363.15 K, Fluid Phase Equilib. 215 (2004) 129–142.
[22] C.M. Kinart, M. Klimczak, A. Ćwiklińska, W.J. Kinart, Densities and excess molar volumes for binary mixtures of some glycols in 2-methoxyethanol at T = (293.15, 298.15 and 303.15) K, J. Mol. Liq. 135 (2007) 192–195.
[23] X.S. Qiao, T.X. Zhao, B. Guo, F. Sha, F. Zhang, X.H. Xie, J.B. Zhang, X.H. Wei, Excess properties and spectral studies for binary system tri-ethylene glycol + dimethyl sulfoxide, J. Mol. Liq. 212 (2015) 187–195.
[24] Y. Chang, J.B. Zhang, Q. Li, L.H. Li, B. Guo, T.X. Zhao, Excess properties and viscous flow thermodynamics of the binary system 1,2-ethanediamine + triethylene glycol at T = (298.15, 303.15, 308.15, and 313.15) K for CO_2 capture, Korean J. Chem. Eng. 31 (2014) 2245–2250.
[25] H. Ghaedi, M. Ayoub, S. Suriati, A.M. Shariff, B. Lal, The study on temperature dependence of viscosity and surface tension of several Phosphonium-based deep eutectic solvents, J. Mol. Liq. 241 (2017) 500–510.
[26] J. Fu, U. Sharma, R. Sparling, N. Cicek, D.B. Levin, Evaluation of medium-chain-length polyhydroxyalkanoate production by Pseudomonas putida LS46 using biodiesel byproduct streams, Can. J. Microbiol. 60 (2014) 461–468.
[27] B. Li, L. Zhao, X.Q. Yue, Y.J. Pang, S. Zhang, Z.J. Wu, J.B. Zhang, Density, viscosity and intermolecular interaction of polyethylene glycol 300 + N, N-dimethylformamide binary mixture, Phys. Chem. Liq. (2020) https://doi.org/10.1080/00319104.2019.1683830.
[28] J.R. Yang, B.S. Zhao, J. Fu, L. Zhao, X.Q. Yue, Y.J. Pang, H.H. Shi, J.B. Zhang, Measurement and relationships of density and viscosity of 1,2-propylene glycol + dimethyl sulfoxide mixtures and spectral insight, J. Mol. Liq. 271 (2018) 530–539.
[29] T.X. Zhao, J.B. Zhang, B. Guo, F. Zhang, F. Sha, X.H. Xie, X.H. Wei, Density, viscosity and spectroscopic studies of the binary system of ethylene glycol + dimethyl sulfoxide at T = (298.15 to 323.15) K, J. Mol. Liq. 207 (2015) 315–322.
[30] M.M. Billah, M.M.H. Rocky, I. Hossain, M.N. Hossain, S. Akhtar, Densities, viscosities, and refractive indices for the binary mixtures of tri-n-butyl phosphate (TBP) with toluene and ethylbenzene between (303.15 and 323.15) K, J. Mol. Liq. 265 (2018) 611–620.
[31] S.K. Begum, R.J. Clarke, M. Shamsuddin Ahmed, S. Begum, M.A. Saleh, Volumetric, viscosimetric and surface properties of aqueous solutions of triethylene glycol, tetraethylene glycol, and tetraethylene glycol dimethyl ether, J. Mol. Liq. 177 (2013) 11–18.
[32] S. Zhang, L. Zhao, X.Q. Yue, B. Li, J.B. Zhang, Density, viscosity, surface tension and spectroscopic studies for the liquid mixture of tetraethylene glycol + N, N -dimethylformamide at six temperatures, J. Mol. Liq. 264 (2018) 451–457.
[33] W.B. Du, X.P. Wang, Density and viscosity for binary mixtures of methyl decanoate with 1-propanol, 1-butanol, and 1-pentanol, J. Mol. Liq. 294 (2019), 111647.
[34] Y. Zhang, J.R. Yang, B. Li, R.M. Zhang, X.H. Xie, J.B. Zhang, Density, viscosity, and spectroscopic and computational analyses for hydrogen bonding interaction of 1,2-propylenediamine and ethylene glycol mixtures, J. Mol. Liq. (2020) https://doi.org/10.1016/j.molliq.2020.112443.
[35] H.H. Shi, L. Ma, B.S. Zhao, Y.J. Pang, Z.J. Wu, Density, viscosity and molecular interaction of binary system tetraethylene glycol + dimethyl sulfoxide at T = (293.15 to 318.15) K, J. Mol. Liq. 250 (2018) 182–191.
[36] M.D.C. Grande, J.A. Julia, M. Garcia, C.M. Marschoff, On the density and viscosity of (water + dimethylsulphoxide) binary mixtures, J. Chem. Thermodyn. 39 (2007) 1049–1056.
[37] Q.G. Zhang, Q. Li, D.Y. Liu, X.Y. Zhang, X.S. Lang, Density, dynamic viscosity, electrical conductivity, electrochemical potential window, and excess properties of ionic liquid N-butyl-pyridinium dicyanamide and binary system with propylene carbonate, J. Mol. Liq. 249 (2018) 1097–1106.
[38] D. Urszula, K. Merta, K. Walczak, Effect of temperature and composition on the density, viscosity surface tension and excess quantities of binary mixtures of 1-ethyl-3-methylimidazolium tricyanomethanide with thiophene, Colloids and Surface, A: Physicochemical and Engineering Aspects 436 (2013) 504–511.
[39] E. Jiménez, H. Casas, A. Luisa Segade, C. Franjo, Surface tensions, refractive indexes and excess molar volumes of hexane + 1-alkanol mixtures at 298.15 K, J. Chem. Eng. Data 45 (2000) 862–866.
[40] L. Zhao, Q. Li, L. Ma, C. Liu, F. Sha, J.B. Zhang, Liquid density, viscosity, surface tension, and spectroscopic investigation of 1,2-ethanediamine + 1,2-propanediol for CO_2 capture, J. Mol. Liq. 241 (2017) 374–385.
[41] X.Q. Yue, L. Zhao, L. Ma, H.H. Shi, T.Y. Yang, J.B. Zhang, Density, dynamic viscosity, excess property and intermolecular interplay studies for 1,4-butanediol + dimethyl sulfoxide binary mixture, J. Mol. Liq. 263 (2018) 40–48.
[42] A.K. Singh, L. Sharma, N. Mallick, J. Mala, Progress and challenges in producing polyhydroxyalkanoate biopolymers from cyanobacteria, J. Appl. Phycol. 29 (2017) 1213–1232.